August 27-31, 2023
FLORENCE - ITALY
ICWE 16
16th International Conference on Wind Engineering

Pressure properties of twisted elliptic cylinders at moderate Reynolds number

Yan-Jiao Guo [1], Xiang-Wei Min [1], Wen-Li Chen [1]

[1] *Harbin Institute of Technology, Harbin, China, fancyjiao@126.com*

SUMMARY:
The twisted elliptic (TE) cylinder is a novel three-dimensional structure with an elliptical cross-section rotating helically in the spanwise direction. This experimental study investigates the surface pressure properties of the TE cylinders at a moderate Reynolds number of 3.8×10^4. Two TE cylinders, denoted as TE11 and TE12, with aspect ratios of 1.1 and 1.2 for elliptical cross-sections, respectively, were selected to compare the performance of vortex shedding suppression. The Gaussian characteristics of the fluctuating pressure at different spanwise positions and the phase difference and coherence function between the pressure signals were analyzed. The results showed that TE12 cylinder was not dominated by antiphase shedding vortices, as in the baseline and TE11 cylinders, but rather by low-frequency components in the flow field. In addition, the fluctuating pressure at the shoulder of TE11 cylinder was negatively skewed, whereas for TE12 cylinder it obeyed a Gaussian distribution owing to the poor contribution of the antiphase shedding vortices.

Keywords: twisted elliptic cylinders, skewness factor, Gaussian characteristics, pressure coherence

1. MOTIVATIONS

The flow around circular cylinders has attracted considerable interest because of the widespread application of cylindrical structures. Meanwhile, control methods that can successfully inhibit vortex shedding from cylinders have been explored. The twisted elliptic (TE) cylinder is a novel three-dimensional structure with an elliptical cross-section rotating helically in the spanwise direction (Jung and Yoon, 2014; Kim et al., 2016; Wei et al., 2016; Yoon et al., 2019). However, previous research on TE cylinders focused on the optimum parameters and vortical structures at low Reynolds numbers. The underlying pressure properties of TE cylinders, such as the Gaussian characteristics, and the phase difference and coherence distribution in the frequency domain, remain unknown. Therefore, this study primarily investigated the surface pressure characteristics of stationary TE cylinders at a moderate Reynolds number of 3.8×10^4.

2. METHODS

The control parameters of the TE cylinders include the major (a) and minor (b) axis radii of the elliptical cross-section and the wavelength (λ), as illustrated in Fig. 1. The distance travelled by the elliptical cross-section rotated by 180° is one wavelength. The ratio of a to b is called the aspect ratio (AR). In this paper, the characteristic length is defined as the hydraulic diameter (D) of the cross-section. According to the work of Kim et al. (2016), the optimum λ/D was found to

be 4.0 at AR = 1.3 and Re = 3.9×10^3, thus, a fixed λ = 4D and two AR values of 1.1 and 1.2 were considered to achieve significant vortex inhibition with the lowest possible AR value. In addition to a standard circular cylinder used as the baseline model, two TE cylinders with AR values of 1.1 and 1.2 termed TE11 and TE12, respectively, were used. The control parameters of all the models are listed in Table 1.

Table 1. Characteristic parameters of all models.

Cases	AR	a /mm	b /mm	D /mm	λ	L
Baseline	1.0	35	35	70	-	8D
TE11	1.1	36.77	33.43	70	4D	8D
TE12	1.2	38.58	32.15	70	4D	8D

The pressure distributions at the midspan of the three models (baseline, TE11, and TE12) were measured. Thirty-two pressure taps were uniformly placed on the middle cross-section, with an interval between adjacent pressure taps of 11.25°. The sample frequency and sample time used for the pressure measurements were 312.5 Hz and 120 s. Considering the periodic variation in the spanwise direction of the TE model, the pressure profiles on different spanwise sections of the TE cylinder were acquired by rotating the model. Five rotation angles (α) were selected: 0°, 22.5°, 45°, 67.5°, and 90°, as shown in Fig. 2.

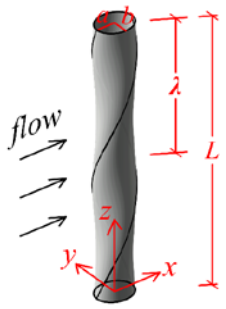

Figure 1. Geometric diagram of TE cylinder.

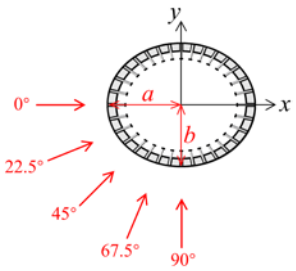

Figure 2. Rotation angle setting for pressure measurement.

3. RESULTS

3.1. Integrated Aerodynamic Forces

The drag and lift forces of the three models at different α values were calculated by integrating the pressure over the model surface. Figure 3 presents the time histories of the lift and drag coefficients of two TE cylinders and the frequency spectra of the lift coefficients. The total aerodynamic coefficient of the TE cylinder was evaluated using a weighted average of the sectional aerodynamic coefficients at the five rotation angles. The RMSs of the lift coefficients for TE11 and TE12 cylinders were 0.098 and 0.027, respectively, which were 77.6% and 93.8% less than those for the baseline cylinder, respectively. In addition, Fig. 3 shows that the St obtained from the dominant vortex shedding frequency (f_s) was approximately 0.2 for TE11 cylinder, which was close to that of the baseline cylinder. However, for TE12 cylinder, the St numbers increased from approximately 0.17 to 0.195 as α increased from (0–67.5°) to 90°.

3.2. Gaussian Characteristics of Fluctuating Pressures

To quantitatively analyze the Gaussian characteristics of the pressure pulsations for the two TE

cylinders, the skewness and kurtosis factors (the third and fourth central moments) of the normalized fluctuating pressures (*NFP*s) at θ = ±90° for all the models are shown in Fig. 4. The skewness and kurtosis factors of the *NFP*s for the baseline cylinder were approximately -0.7 and 3.5, respectively, which were significantly different from 0 and 3 of the Gaussian distribution. The skewness values of the *NFP*s for TE11 cylinder increased by 0.1-0.2 at five α values. However, their kurtosis values were close to or even larger than those of the baseline cylinder. For TE12 cylinder, the skewness and kurtosis values of the pressure distributions approached 0 and 3, respectively, at all α values.

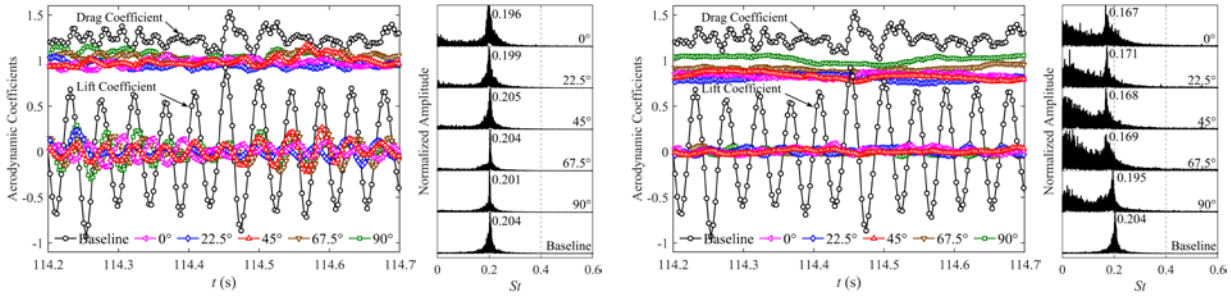

(a) TE11 (b) TE12

Figure 3. Time histories of aerodynamic coefficients and frequency spectra of lift coefficients for TE cylinders at different rotation angles.

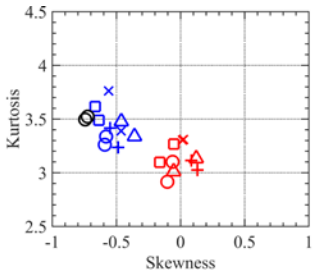

Figure 4. Skewness and kurtosis values of fluctuating pressures at θ = ±90°: black marker, baseline; blue marker, TE11; red marker, TE12; for TE cylinders: ×, α = 0°; +, α = 22.5°; △, α = 45°; □, α = 67.5°; ○, α =90°.

3.3. Phase Difference and Coherence Properties of Fluctuating Pressures

To determine the coupling between the pressure signals at opposing angles, we extracted the magnitude-squared coherence (*COH*) and phase difference ($\Delta\phi$) between the pressure signals p(±90°) at each frequency. The *COH* is a function of frequency (f) and is calculated from the respective power spectral densities (S_{XX} and S_{YY}) and the cross power spectral density (S_{XY}) of two signals (X and Y), as shown in Eq. (1).

$$COH(f) = \frac{|S_{XY}(f)|^2}{S_{XX}(f)S_{YY}(f)} \tag{1}$$

The phase difference $\Delta\phi$ between the two signals at the strong-coherence frequency is the angle of the cross-spectrum at that frequency. The coherence and phase difference functions of the *NFP*s at θ=±90° for all models are shown in Fig. 5. The pressure pulsations of the baseline

cylinder exhibited a significant coherence of approximately 1 and a phase difference of 180° at St=0.203, implying that alternatively shed vortices provided energy for the lift fluctuations.
The pressure coherent feature of TE11 cylinder was similar to that of the baseline cylinder. The frequency range with a strong coherence broadened in the low-frequency region and narrowed near f_s. As for TE12 cylinder, it was evident that the coherence factors between the fluctuating pressures p(±90°) at all rotation angles were significantly larger in the low-frequency region than those near the f_s. In addition, the frequency range with strong coherence near f_s was reduced by half, indicating that little pressure pulsation energy was provided near f_s. Therefore, TE12 cylinder was not dominated by antiphase shedding vortices, as in the baseline and TE11 cylinders, but rather by inphase low-frequency components in the flow field.

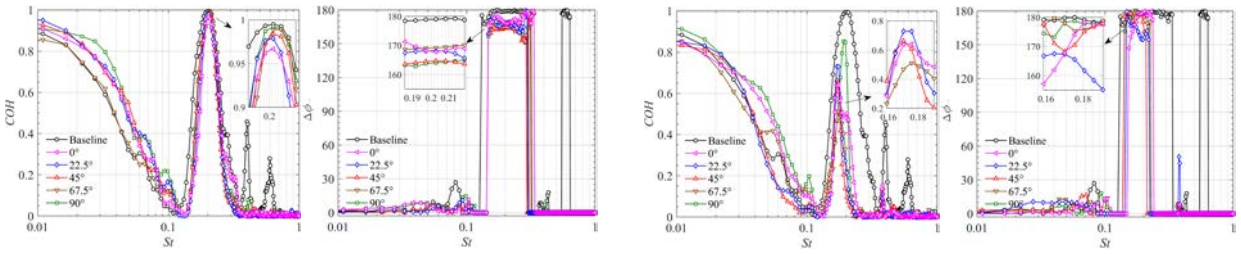

(a) TE11 (b) TE12

Figure 5. Phase difference and coherence properties of normalized fluctuating pressures at θ = ±90°.

4. CONCLUSIONS

Two TE cylinders, denoted as TE11 and TE12, with AR values of 1.1 and 1.2 were selected to reveal the underlying pressure properties at Re=3.8×10^4. The RMS lift force was reduced by 77.6% and 93.8% for TE11 and TE12 cylinders, respectively, compared with the baseline cylinder. Owing to the strong coherent antiphase shedding vortices, the fluctuating pressure at the shoulder of TE11 cylinder was negatively skewed and exhibited the same non-Gaussian characteristics as those of the baseline cylinder. However, as the AR increased to 1.2, the coherence between the fluctuating pressures p(±90°) was larger in the low-frequency region than near f_s. The fluctuating pressure of TE12 cylinder obeyed a Gaussian distribution owing to the poor contribution of the antiphase shedding vortices.

ACKNOWLEDGEMENTS

This work was supported by the National Natural Science Foundation of China through Grants U2106222, 52008140, and 51978222.

REFERENCES

Jung, J. H. and Yoon, H. S., 2014. Large eddy simulation of flow over a twisted cylinder at a subcritical Reynolds number. Journal of fluid mechanics, 759, 579-611.

Kim, W., Lee, J., and Choi, H., 2016. Flow around a helically twisted elliptic cylinder. Physics of Fluids, 28(5), 053602.

Wei, D. J., Yoon, H. S., and Jung, J. H., 2016. Characteristics of aerodynamic forces exerted on a twisted cylinder at a low Reynolds number of 100. Computers and Fluids, 136, 456-466.

Yoon, H. S., Kim, M. I., and Kim, H. J., 2019. Reynolds number effects on the flow over a twisted cylinder. Physics of Fluids, 31(2), 025119.